Broadband Distributed-Feedback Quantum Cascade Laser Array Operating From 8.0 to 9.8 um

Broadband Distributed-Feedback Quantum Cascade Laser Array Operating From 8.0 to 9.8 μm

Benjamin G. Lee, Haifei A. Zhang, Christian Pflügl, Laurent Diehl, Mikhail A. Belkin, Milan Fischer, Andreas Wittmann, Jerome Faist, and Federico Capasso

***Abstract*—An ultra-broadband distributed-feedback quantum cascade laser array was fabricated, using a heterogeneous cascade based on two bound-to-continuum designs centered at 8.4 and 9.6 μm. This array emitted in a range over 220 cm^{-1} near a 9-μm wavelength, operated in pulsed mode at room temperature. The output power of the array varied between 100- and 1100-mW peak intensity.**

***Index Terms*—Distributed-feedback (DFB) lasers, infrared spectroscopy, mid-infrared, quantum cascade lasers (QCLs), semiconductor lasers.**

I. Introduction

QUANTUM cascade lasers (QCLs) are semiconductor lasers based on resonant tunneling and optical transitions between electronic levels within the conduction band of a multiquantum-well structure. As a result, the emitted photon energy is determined by the thicknesses of the wells and barriers and can be tailored by bandgap engineering. The emission wavelengths of mid-infrared QCLs span from 3 to 24 μm [1] and cover the "fingerprint" region of molecular absorption. This makes QCLs particularly interesting for spectroscopic applications [2]. QCLs can achieve watt-level output power in continuous-wave operation at room temperature (RT) [3], [4] and can be designed with broadband gain, with full-width at half-maximum (FWHM) of more than 350 cm^{-1}, enabling wide wavelength tunability [5].

Arrays of distributed-feedback (DFB)-QCLs can be made as single-mode sources covering a wide range of mid-infrared frequencies [6], [7], with potential applications in spectroscopy. In our previous work [6], we demonstrated a proof-of-concept DFB-QCL array, which achieved single-mode lasing coverage of 85 cm^{-1} near 9-μm wavelength. We used a bound-to-continuum active region design, which has inherently broad gain with an FWHM of nearly 300 cm^{-1}, as demonstrated by [8]. We did not attempt to cover the entire range of the gain spectrum with DFB-QCLs in our first attempt.

Manuscript received February 17, 2009; revised March 25, 2009. Current version published June 17, 2009. This work was supported by the DARPA Optofluidics Center under Grant HR001-04-1-0032 and by MIT Lincoln Laboratory with Department of Defense Award FA872-05-C-0002.

B. G. Lee, H. A. Zhang, C. Pflügl, L. Diehl, and F. Capasso are with the School of Engineering and Applied Sciences, Harvard University, Cambridge, MA 02138 USA (e-mail: capasso@seas.harvard.edu).

M. A. Belkin was with Harvard University, Cambridge, MA 02138 USA, and is now with the University of Texas at Austin, Austin, TX 78712 USA.

M. Fischer, A. Wittmann, and J. Faist are with ETH Zurich, Zurich 8093, Switzerland.

Digital Object Identifier 10.1109/LPT.2009.2020440

Since it is advantageous for chemical sensing to have broadband single-mode laser sources, we are interested in increasing the range of frequencies that can be covered by a single DFB-QCL array. We chose, therefore, to use an active region design with an even broader gain spectrum, and we aim to space the design frequencies of our DFB-QCLs so that they span over the entire gain spectrum available.

An ultra-broadband laser was first demonstrated by [9], accomplished by using a heterogeneous cascade to support lasing over a broad range of frequencies. [5] employed a heterogeneous cascade of two bound-to-continuum designs (with individual gain maxima at 8.4 and 9.6 μm) to achieve a gain spectrum with a record FWHM of 350 cm^{-1}. Using this "two-stack" bound-to-continuum QCL, [10] obtained a single-mode tuning range of 292 cm^{-1} in an external-cavity (EC) setup. Here, we will employ the same two-stack active region design to achieve an ultra-broadband DFB-QCL array.

II. Device Design and Fabrication

The QCL material used to fabricate the laser array was grown by molecular beam epitaxy. The structure grown consists of a bottom waveguide cladding of 2 μm of InP-doped 1×10^{17} cm^{-3}, followed by 200 nm of InGaAs-doped 3×10^{16} cm^{-3}, a first active region which is 1.4 μm thick, 100 nm of InGaAs-doped 3×10^{16} cm^{-3}, a second active region which is 1.3 μm thick, and 600 nm of InGaAs-doped 3×10^{16} cm^{-3}. The first active region consists of 20 stages based on a bound-to-continuum design emitting at $\sim$9.6 μm. The second active region is 20 stages of a bound-to-continuum design at 8.4 μm. The design of the two active regions is outlined in [5]. The structure was grown without an upper cladding, since it was anticipated that DFB gratings would be fabricated in the top 600-nm-thick InGaAs layer.

We processed mesa structures to measure the luminescence of the QCL material and to determine the gain spectrum. Circular mesa structures with 200-μm diameter were fabricated and then the samples were cleaved to split the mesas into semicircles, with an exposed facet where the luminescence could be measured. The luminescence was measured pulsed at 80 kHz at RT, with long pulses corresponding to a duty cycle of 5%. From the luminescence we determined that the gain spectrum has an FWHM of over 350 cm^{-1}, centered at around 1150 cm^{-1}.

We chose to design an array of DFB-QCLs to cover the spectral range from 1000 to 1310 cm^{-1}, with laser emission frequencies spaced regularly by $\sim$10 cm^{-1}. This was done to cover the central portion of the measured luminescence spectrum. By simulating the waveguide structure of the QCL, we obtained an effective refractive index of 3.19 for the TM_{00} mode. Assuming

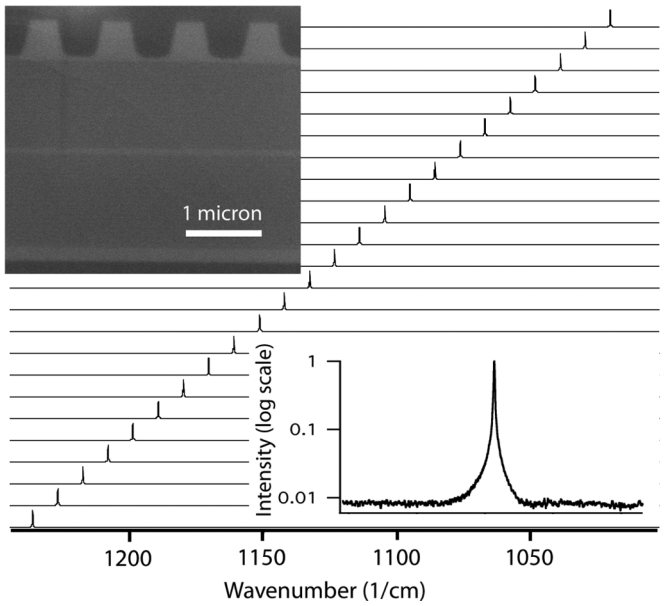

Fig. 1. Spectra of 24 single-mode DFB lasers in the array. Laser frequencies are spaced $\sim$9.5 cm^{-1} apart and span a range of $\sim$220 cm^{-1}. (Inset, top left) Scanning electron micrograph showing a cross-section of the device, which has been cut along the laser ridge. The grating corrugation can be seen as the rectangular wave near the top of the image, and the two active regions are below, with a thin InGaAs spacer between them. (Inset, bottom right) Spectrum of a representative laser in the array on a log scale, showing sidemode suppression $>$20 dB.

this effective refractive index, we chose the grating periods to range between 1.197 and 1.567 μm, corresponding to the desired emission frequencies between 1000 and 1310 cm^{-1}.

Device processing began with the fabrication of an array of 32 buried DFB gratings in the QCL material. We chose to have deeply etched, buried gratings in order to have a large grating coupling constant κ. This is done to facilitate the fabrication of strongly over-coupled DFBs, having $\kappa L \gg 1$, where L is the DFB's length. Strongly over-coupled DFB-QCLs have better (longitudinal) single-mode selection—this refers to the yield of single-mode DFBs lasing at the desired frequencies, and is a very important consideration for arrays of DFBs. The topic of (longitudinal) single-mode selection for DFB-QCLs is discussed in detail in [7].

To fabricate the buried gratings, a 200-nm-thick layer of Si_3N_4 was deposited on top of the exposed top InGaAs by chemical vapor deposition. First-order Bragg gratings (with periodicities as mentioned above) were exposed onto PMMA using an Elionix ELS-7000 100-keV electron beam lithography system. This pattern was transferred into the Si_3N_4 by using a CF_4-based dry-etch. The gratings were then etched 590 nm deep into the InGaAs layer with a HBr–BCl_3–Ar–CH_4 plasma in an inductively coupled plasma reactive ion etching machine (ICP-RIE) (Fig. 1, top left inset). A top cladding consisting of 2 μm of InP-doped 5×10^{16} cm^{-3} and 500 nm of InP-doped 5×10^{18} cm^{-3} was regrown over the gratings using metal–organic vapor phase epitaxy. The real part of the grating coupling strength was obtained by simulating the DFB modes and calculating the photonic gap between the two primary modes supported by the grating. The coupling coefficient (real part) is then given by $\kappa \sim 42$ cm^{-1}.

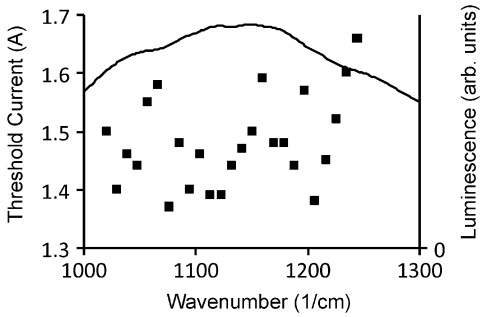

Fig. 2. Plot of the threshold current required for lasing, as a function of the laser frequency. This plot is overlaid on the electroluminescence of a mesa structure fabricated from the QCL wafer, showing the gain spectrum of the material. The mesa was pumped with a 9-V pulse at 80 kHz at RT, with a 5% duty cycle.

Laser ridges, 15 μm wide and spaced 75 μm apart, were defined on top of the buried gratings by dry-etching the surrounding areas 9 μm deep with a HBr–BCl_3–Ar–CH_4 plasma using ICP-RIE. During this step, the back facet of the lasers was also defined. The bottom and the sidewalls of the laser ridges were insulated by Si_3N_4 and a 600-nm-thick gold top contact was deposited. Using Si_3N_4 insulation on the ridge sidewalls helps ensure single-tranverse mode lasing, as Si_3N_4 is highly absorbing at these wavelengths, thus suppressing higher-order lateral modes of the ridge waveguide. The samples were then thinned to 200 μm and a metal bottom contact was deposited. Finally, the front facets of the lasers were defined by cleaving to obtain 2-mm-long lasers and the laser array was indium-soldered onto a copper block for testing. The facets were left uncoated. The entire DFB laser array chip is only 4 mm by 5 mm in size.

III. Performance

All 32 lasers in the array were individually tested using a probe station at RT. The lasers were tested in pulsed mode with 50-ns pulses at a repetition rate of 80 kHz. Lasing was observed from 25 out of the 32 lasers, with all operating devices being single-mode (Fig. 1). Lasing was not observed from lasers at the high-frequency end of the array, likely because there was insufficient gain at those frequencies, which are towards the edge of the gain spectrum. We can plot the threshold currents for the DFB lasers in the array (Fig. 2), which ranged from 1.37 to 1.66 A, corresponding to current densities of 4.6 to 5.5 kA/cm^2. While there is significant scatter in the points, the data suggests that there is an increase in the threshold for lasers near the high-frequency edge of the array.

The lasing frequencies of the QCLs in the array were spaced $\sim$9.5 cm^{-1} apart and spanned from 1020 to 1245 cm^{-1} (8.0- to 9.8-μm wavelength). The small difference between calculated and measured frequencies is most likely due to our inexact knowledge about the precise material refractive indices when we performed the simulations. The laser emitting at 1245 cm^{-1} had a high threshold (close to the rollover point) and only lased weakly before turning off at higher currents; its spectrum is noisy due to the low signal level, and is not shown in the plot. All the other DFB lasers remained single-mode with $>$20-dB sidemode suppression up to at least 2.0 A in current (Fig. 1, bottom right inset). Subthreshold measurements revealed the bandgap

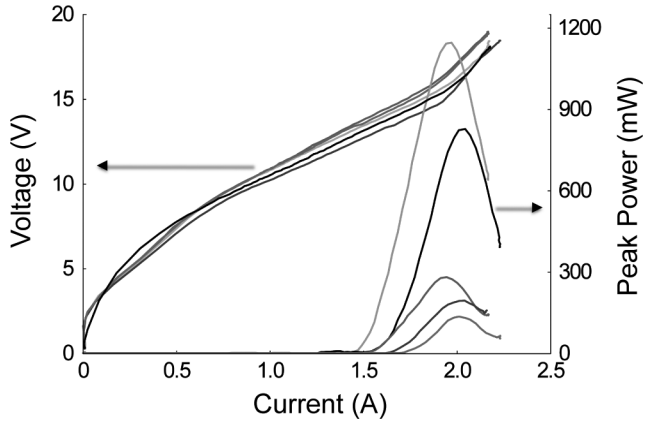

Fig. 3. Plot of the voltage (left axis) and light output (right axis) characteristics of several representative lasers in the array as functions of current. There is large variability in the output power of different lasers in the array. In ascending order of peak output power, the plot shows the light output of lasers in the array having emission frequencies of 1170, 1067, 1113, 1160, and 1104 cm^{-1}.

of the DFB grating to be 4.5 cm^{-1}, giving a coupling strength per unit length of $\kappa \approx 45\ \text{cm}^{-1}$, in agreement with our calculations. With the lasers being 2 mm long, the DFBs are strongly over-coupled with $\kappa L \sim 9$.

All the lasers were lasing on the same side of the DFB's photonic gap, specifically in the DFB mode that is on the high-frequency side of the gap. We attribute the good (longitudinal) single-mode selection to the fact that the lasers are strongly over-coupled and contain a small amount of loss-coupling ($\sim$0.05 cm^{-1}), as in our previous work [7].

We note that the overall tuning range of the DFB-QCL array, 225 cm^{-1}, is less than the 292 cm^{-1} achieved for EC-QCLs by [10]. The lower waveguide losses of their QCLs is the likely reason. They employed low-loss buried-heterostructure QCLs which also improve heat dissipation; by contrast, our lasers were configured as narrow etched-ridge lasers, with the sidewalls insulated using Si_3N_4, which absorbs significantly at wavelengths around 9 μm.

Next we examine the output power and current–voltage (I–V) characteristics of devices in the array, shown in Fig. 3. There were small differences in the I–V curves of the lasers resulting from the varying series resistances of different length gold contacts running between the laser ridges and the wire-bond pads on the QCL array chip. We also observed a large variation in the slope efficiency of the lasers between 250 and 2500 mW/A. The variation in slope efficiency is likely due to the random variation in the position of the end mirror facets relative to the laser ridge gratings. As shown in [11], the variation in the position of the laser facet alters the distribution of light intensity within the laser cavity, which results in a variation in the amount of light emitted from a facet. This effect for arrays of DFB-QCLs is discussed in detail in [7].

The potential for crosstalk between different lasers in the array is not a concern, as the lasers are meant to be used in an alternating fashion. For spectroscopic applications, only a single laser would be turned on at any particular moment.

IV. Conclusion

We have demonstrated a broadband DFB-QCL array covering over 220 cm^{-1} around 9-μm wavelength; this range is nearly 20% of the center frequency. The broad coverage was made possible by using a gain element with a heterogeneous cascade providing a wide gain spectrum with FWHM $> 350\ \text{cm}^{-1}$. We achieved a significant increase in coverage from our previous results [6] where we demonstrated an array spanning $\sim$85 cm^{-1}. We envision that broadband DFB-QCL arrays will be used in spectroscopic applications where it is desirable to monitor different widely spaced spectroscopic features. In the future, we hope to integrate DFB-QCL arrays into a variety of spectroscopic devices, including portable mid-infrared spectrometers.

Acknowledgment

The authors gratefully acknowledge the Center for Nanoscale Systems (CNS) at Harvard University. Harvard-CNS is a member of the National Nanotechnology Infrastructure Network (NNIN).

References

[1] F. Capasso, C. Gmachl, D. L. Sivco, and A. Y. Cho, "Quantum cascade lasers," *Phys. Today*, vol. 55, pp. 34–40, May 2002.

[2] A. Kosterev and F. Tittel, "Chemical sensors based on quantum cascade lasers," *IEEE J. Quantum Electron.*, vol. 38, no. 6, pp. 582–591, Jun. 2002.

[3] Y. Bai, S. R. Darvish, S. Slivken, W. Zhang, A. Evans, J. Nguyen, and M. Razeghi, "Room temperature continuous wave operation of quantum cascade lasers with watt-level optical power," *Appl. Phys. Lett.*, vol. 92, pp. 101105-1–101105-3, 2008.

[4] A. Lyakh, C. Pflugl, L. Diehl, Q. J. Wang, F. Capasso, X. J. Wang, J. Y. Fan, T. Tanbun-Ek, R. Maulini, A. Tsekoun, R. Go, and C. Kumar N. Patel, "1.6 W high wall plug efficiency, continuous-wave room temperature quantum cascade laser emitting at 4.6 μm," *Appl. Phys. Lett.*, vol. 92, pp. 111110-1–111110-3, 2008.

[5] R. Maulini, A. Mohan, M. Giovannini, J. Faist, and E. Gini, "External cavity quantum-cascade lasers tunable from 8.2 to 10.4 μm using a gain element with a heterogeneous cascade," *Appl. Phys. Lett.*, vol. 88, pp. 201113-1–201113-3, 2006.

[6] B. G. Lee, M. A. Belkin, R. Audet, J. MacArthur, L. Diehl, C. Pflugl, D. Oakley, D. Chapman, A. Napoleone, D. Bour, S. Corzine, G. Hofler, J. Faist, and F. Capasso, "Widely tunable single-mode quantum cascade laser source for mid-infrared spectroscopy," *Appl. Phys. Lett.*, vol. 91, pp. 231101-1–231101-3, 2007.

[7] B. G. Lee, M. Belkin, C. Pflugl, L. Diehl, H. A. Zhang, R. M. Audet, J. MacArthur, D. Bour, S. Corzine, G. Hofler, and F. Capasso, "DFB quantum cascade laser arrays," *IEEE J. Quantum Electron.*, vol. 45, no. 5, pp. 554–565, May 2009.

[8] R. Maulini, M. Beck, J. Faist, and E. Gini, "Broadband tuning of external cavity bound-to-continuum quantum-cascade lasers," *Appl. Phys. Lett.*, vol. 84, pp. 1659–1661, 2004.

[9] C. Gmachl, D. L. Sivco, R. Colombelli, F. Capasso, and A. Y. Cho, "Ultra-broadband semiconductor laser," *Nature*, vol. 415, pp. 883–887, Feb. 2002.

[10] A. Wittmann, A. Hugi, E. Gini, N. Hoyler, and J. Faist, "Heterogeneous high-performance quantum-cascade laser sources for broad-band tuning," *IEEE J. Quantum Electron.*, vol. 44, no. 11, pp. 1083–1088, Nov. 2008.

[11] W. Streifer, R. Burnham, and D. Scifres, "Effect of external reflectors on longitudinal modes of distributed feedback lasers," *IEEE J. Quantum Electron.*, vol. 11, no. 4, pp. 154–161, Apr. 1975.